Diagnostic Tool to Detect Electrode Flooding in Proton-Exchange-Membrane Fuel Cells

Wensheng He, Guangyu Lin, and Trung Van Nguyen
Chemical and Petroleum Engineering Dept., The University of Kansas, Lawrence, KS 66045

An electrode flooding monitoring device designed for PEM fuel cells with interdigitated flow distributors was proposed and tested. The pressure drop between the inlet and outlet channels can be used as a diagnostic signal to monitor the liquid water content in the porous electrodes, because of the strong dependence of the gas permeability of the porous electrodes on liquid water content. It can be used with no modification to existing fuel-cell assembly to give real-time flooding information in the electrode backing layers during operation. The device has been employed to investigate the correlation between the fuel-cell performance and the liquid water saturation level in the backing layers, the effects of various operating parameters, and the dynamics and hysteresis behavior of liquid water in the backing layers. The results provide, for the first time, direct evidence to show that inadequate water removal causes liquid water build up in the cathode, which in excessive amounts can severely reduce the performance of a PEM fuel cell. It was observed that more than 30 min. were needed for a PEM fuel cell to reach a new steady state when subjected to current-density changes, and this was attributed to the slow liquid water transport process. The results confirmed that increasing air flow rate or cell temperature increased the liquid water removal rate from the backing layers. The hysteresis behavior of fuel-cell performance was related to the water imbibition and drainage cycles in the electrode backing layers and was attributed to the difference in the water removal rate by capillary force and the difference in membrane conductivity.

Introduction

The proton exchange membrane (PEM) fuel-cell system is being considered as a power source for electric vehicles, residential power and a variety of portable electrical devices, because of its high efficiency, simplicity in design and operation, and environmentally friendly characteristics. However, for this PEM system to be cost effective for use in these applications, its performance and efficiency need to be improved further. A better understanding of the phenomena occurring in the electrodes of the fuel cells, especially the performance and efficiency-limiting processes, is essential for achieving this goal.

Of the performance-controlling components in the PEM fuel cell, the cathode is most influential. The oxygen-reduction rate at the cathode being the limiting kinetic step determines how much current can be generated. During operation, the cathode becomes flooded when the water generation rate at the cathode by electroosmotic drag and the oxygen-reduction reaction exceeds the water removal rate from the cathode by back-diffusion to the anode, evaporation, water-vapor diffusion, and capillary transport of liquid water through the cathode backing layer. Figure 1 shows the cell voltage and the voltage losses due to individual components as a function of current density obtained for a PEM fuel cell operating on hydrogen and oxygen at 40°C with interdigitated flow fields. The voltage losses of individual cell components were obtained using the reference electrode arrangement also shown in Figure 1.

Note that the voltage loss associated with the cathode constitutes a major portion of the total voltage losses in a PEM

Correspondence concerning this article should be addressed to T. V. Nguyen.

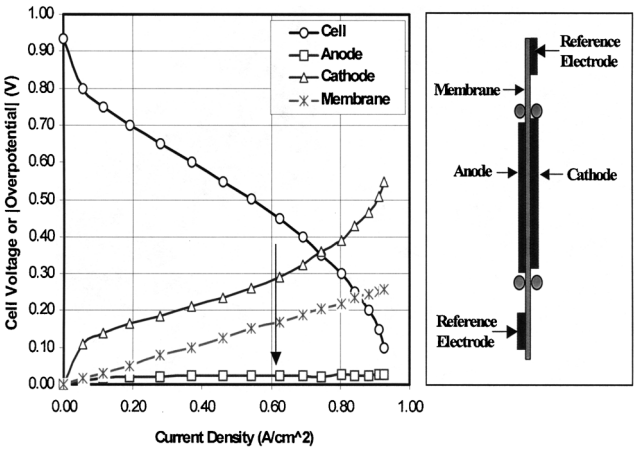

Figure 1. Voltage losses by individual components in a PEM fuel cell obtained using a fuel cell with reference electrodes.

fuel cell during operation. The large voltage loss observed for the cathode is attributed to the slow oxygen-reduction reaction kinetics, which are several orders of magnitude slower than that of hydrogen oxidation. Beyond a certain current density the water generation rate by electroosmotic drag and the oxygen-reduction reaction exceeds the water removal rate from the cathode catalyst and backing layers, and electrode flooding occurs. When the cathode becomes flooded with liquid water, the transport rate of oxygen to the catalyst sites in the cathode is greatly reduced, and the oxygen-reduction rate becomes mass-transport-limited, giving rise to the rapid increase in the cathode overpotential, and consequently a sharp decrease in the cell voltage, as shown in Figure 1. For the fuel cell and the conditions used in our laboratory, this point is marked by the arrow in Figure 1.

To minimize the effect of electrode flooding, interdigitated flow distributors are employed in some PEM fuel cells (Nguyen, 1996; Wood et al., 1998; He et al., 2000). As shown in Figure 2 this flow-field design has dead-ended gas channels that force the incoming gas to flow through the porous backing layer to exit. The convective gas flow provides more effective gas transport and liquid water removal from the electrodes. In addition to evaporation and back diffusion through the membrane, liquid water can also be removed by

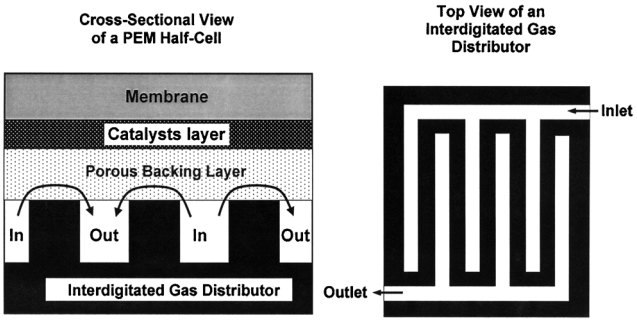

Figure 2. A PEM fuel cell with an interdigitated gas distributor; the arrows show the direction of the convective gas flow.

the shear drag force of the convective gas flow. Note also that when direct liquid water injection is used for anode humidification, the anode could also be flooded if excessive liquid water is injected (Wood et al., 1998; Nguyen and White, 1993). Direct liquid-water injection provides both anode gas humidification and evaporative cooling of the fuel cell. When the interdigitated flow field is used with direct liquid-water injection, the shear drag force of the convective gas flow prevents excessive liquid-water from being entrapped in the gas diffusion layer, thus preventing electrode flooding in the anode.

To evaluate various water-management strategies and to identify the most efficient one, one needs a diagnostic tool that can measure the extent of electrode flooding in the fuel cell and the relative rates of different water-transport mechanisms. However, to the best of our knowledge no existing diagnostic tool can provide direct information on the flooding level in the gas diffusion layers in the fuel cell during operation. Recently, our research group has shown that the pressure drop between the inlet and outlet of the fuel cell can be used as a diagnostic signal to monitor the extent of electrode flooding in a PEM fuel cell using the interdigitated flow fields (Nguyen et al., 2001; He and Nguyen, 2002). Since the gas has to flow through the porous backing layers when the interdigitated flow field is used, the pressure drop across the cell is controlled predominantly by the pressure drop caused by the convective gas flow through the porous backing layers, assuming negligible pressure drop along the channels. The pressure drop due to gas flow through the porous backing layers is governed by the velocity and viscosity of the gas and the morphological properties of the backing layer that affect the transport of the gas.

For two-phase flow through a porous medium, the pressure drop across this medium is proportional to the gas velocity and viscosity, and inversely proportional to the gas permeability in the porous medium (Whitaker, 1986). The gas permeability in this case is a strong function of the liquid-water saturation level in the porous medium. The presence of liquid water in the porous medium reduces the cross-sectional area available in the porous medium for the gas flow. As a result, the flow resistance for the gas phase increases, which in turn causes the gas velocity to decrease for a given pressure drop. Similarly, for a given gas velocity the presence of liquid water in the porous medium causes the pressure drop to increase due to increased flow resistance. Because the pressure drop between the inlet and outlet of a fuel cell using interdigitated flow fields is very sensitive to the amount of liquid water existing in the backing layers, it can be used to determine (1) the liquid saturation level or liquid water flooding level in the electrode backing layers during operation, and (2) its effect on the fuel-cell performance.

The relationship between the gas permeability and the liquid water saturation level is required for quantitative analysis. General, semi-empirical correlations between gas permeability and liquid water content have been established for various porous media (Kaviany, 1995). For carbon paper and carbon cloth that are typically used as the electrodes backing layers in PEM fuel cells, several modeling studies of two-phase flow in PEM fuel cells have assumed some form of relationship between gas permeability and liquid water content (He et al., 2000; He and Nguyen, 2002; Natarajan and

Nguyen, 2001; Wang et al., 2001). However, no experimental study has been conducted to verify those assumptions due to the difficulties associated with measuring the water saturation level in these diffusion layers.

An experimental method is currently being developed in our laboratory to investigate the dependence of the gas relative permeability on the liquid-water saturation level in backing layer materials commonly used in PEM fuel cells. Knowledge of the exact functionality of gas permeability is critical for quantitative analysis of liquid-water content in the backing layers. The knowledge gained from the work will help identify morphological and wetting properties that will result in lower electrode flooding and higher fuel-cell performance.

The objective of this article is to establish the pressure-drop measurement as a diagnostic tool that can be used to determine the effects of liquid-water flooding in the electrode backing layers on the performance of PEM fuel cells with interdigitated flow fields.

Experimental

Two pressure sensors (MPXM 2053GS by Motorola) were placed in the hydrogen and air feed lines at the inlets of the anode and cathode of a PEM fuel cell. The outlets of the cell were exhausted to atmosphere. The pressure sensors have a full range of 50 kPa, with a resolution of 0.01 kPa and an accuracy of 0.20 kPa. The fuel-cell testing system and setup were typical otherwise. Interdigitated flow fields were used in both the anode and cathode. It was experimentally verified that the pressure drops in the main feed lines, the flow channels, and the exhaust lines were negligible for the flow rates studied here to confirm that the total pressure drops measured represent the pressure drops across the backing layers. The pressure drops, cell voltages, and currents were recorded by a data-acquisition system.

The membrane/electrode assemblies (MEAs) used in this study were made in our laboratory, using E-Tek 20% Pt/C catalysts, E-Tek 30% wet-proof Toray paper for the backing layers, and Nafion 112 membrane. Electrodes were prepared by spraying catalyst ink (Pt/C catalysts mixed with Nafion solution) onto the backing layers. The electrodes were hot-pressed onto the membrane to form the MEAs. The active areas of the MEAs were 1.1 cm^2 and the catalyst loadings on the MEAs were about 0.35 mg-Pt/cm^2/electrode.

The cell temperature was controlled at a given setpoint within ± 0.5°C. Hydrogen and air feed streams were humidified using sparging bottles. Other operating conditions like hydrogen and air flow rates will be given later for each experimental case study. The cell was operated mostly under constant-cell-voltage mode. To generate a polarization curve, the cell was tested under constant voltage mode, and the cell voltage was varied from open circuit to 0.3 V at 0.05-V intervals. The cell was held at each voltage interval for 5 min. The current densities used to generate the polarization curve were averaged over these 5-min. intervals.

Results and Discussion

Cathode flooding and cell performance

It had long been suspected that cathode flooding was the major cause of poor fuel-cell performance at high current densities under normal operating conditions. However, no direct experimental proof was available due to the lack of proper diagnostic tools. Now, armed with the pressure-drop signal, we can correlate the pressure drops, which reflect the electrode flooding level, with the cell performance, use this information to identify the operating conditions and electrode properties and design that lead to electrode flooding, and develop solutions to this problem. The first concrete evidence that electrode flooding in the cathode is the cause of poor fuel-cell performance at high current densities is given in Figure 3.

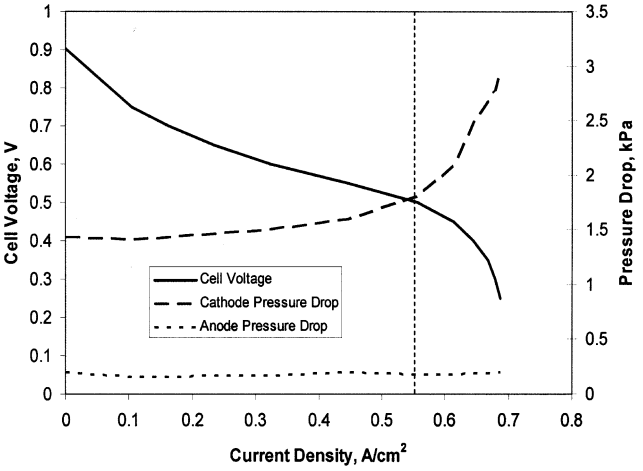

Figure 3. Effect of cathode flooding on a PEM fuel-cell performance.

Cell temperature: 51°C; H_2 flow rate: 2.0 A/cm^2; air flow rate: 2.8 A/cm^2; ambient pressure; H_2 sparger temperature: 50°C; air sparger temperature: 27°C.

The results presented in Figure 3 can be divided into two regions, one for current densities from 0 to 0.55 A/cm^2, and the other for those beyond 0.55 A/cm^2, as marked by the dashed line. Note that as the cell current density increased from 0 to 0.55 A/cm^2, the cell voltage decreased, as expected, due to activation and ohmic losses in the fuel cell. During this time, the pressure drop in the cathode increased from 1.37 kPa to 1.71 kPa, while the anode pressure drop remained essentially constant at 0.18 kPa. The higher pressure drop in the cathode relative to that in the anode is attributed to three main factors: (1) higher volumetric flow rate when air is used; (2) air has higher viscosity than hydrogen; and (3) liquid water remaining in the cathode backing layer from the previous run. The small pressure-drop increase on the cathode side can be attributed to the additional net mass generated in the gas phase on the cathode side by the production of water vapor by the oxygen-reduction reaction and electroosmotic process.

Next, as the current density increased beyond 0.55 A/cm^2, the cell voltage decreased rapidly, and this rapid drop in cell voltage corresponded to a rapid increase in the gas pressure drop across the cathode backing layer. Note that pressure drop on the anode side continued to remain constant. A fuel cell is said to have reached its mass-transport-limited condition when this rapid drop in the cell voltage occurred, and this mass-transport limitation had been attributed to the mass-transport rate of oxygen to the catalyst sites reaching a

limit. These results clearly support our previous claim that the oxygen transport rate in the cathode should be able to support much higher current densities than normally observed in PEM fuel cells and that it is the presence of liquid water in the cathode backing layer that blocks the gas pores that limits the transport of oxygen, and, hence, reduces the cathode and fuel-cell performance (Yi and Nguyen, 1995).

The flooding effects are more pronounced in this study, because the cell temperature for all the experiments in this study was below 60°C. The results obtained in this study would be valuable for PEM fuel cells that need frequent startup and shutdown and experience transient temperature cycles due to the change of loads, as in, for example, portable or automobile applications.

Liquid-water dynamics in a PEM fuel cell

This experiment was conducted to investigate a previous observation that a PEM fuel cell reached a new steady-state current density much quicker when it operated at low current densities than when it operated at high current densities. We had suspected this slow response at high current densities was due to the dynamics and slow transport rate of liquid water in the cathode backing layer and wanted to use this new diagnostic tool to confirm the root causes of this phenomenon.

In this experiment, the fuel cell was tested at 35°C and under constant voltage mode. The cell was first held at open circuit for one hour. Then the cell was stepped from open circuit to 0.5 V and held at this voltage long enough for the current density to reach steady state. Once this was achieved, the cell was stepped back to open circuit and held there for another 90 min., and the same cycle was repeated again. Results for the two cycles are presented in Figure 4.

Note that since the cathode and anode were relatively dry when the experiment started, no changes in the pressure drops in the cathode and anode were observed during the first hour while the cell was at open circuit. Next, as soon as the cell voltage was stepped to 0.5 V, the current density increased to 0.42 A/cm^2, dropped quickly in the first 10 min. to 0.35 A/cm^2, and then slowly leveled out at 0.3 A/cm^2 after about 30 min. In the same period, the cathode pressure drop increased sharply from 0.48 kPa to 4.14 kPa, and then leveled out at the same pressure drop with some minor oscillations as the current density began to level out. This sharp increase in the cathode pressure drop is attributed to liquid water accumulating in the backing layer and the catalysts layer of the cathode. The minor oscillations in the pressure drop are caused by liquid water being flushed out and reaccumulated in the backing layer due to the complicated interaction between the capillary force, pressure gradient, and gas drag force. The oscillations could also be attributed to the redistribution of liquid water within the backing layer due to nonuniform permeability and capillary property of the porous medium.

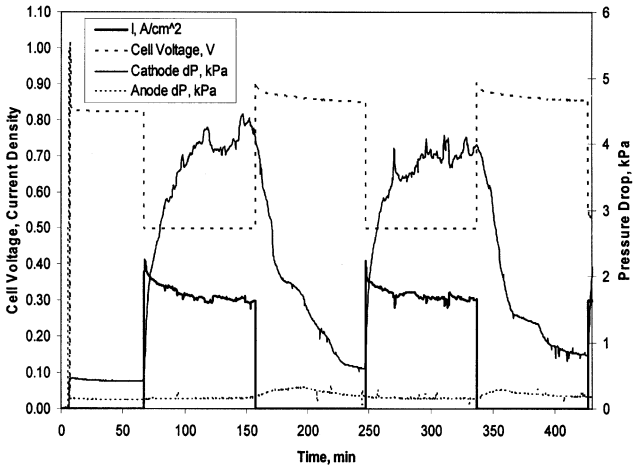

Figure 4. Current density and cathode pressure drop responses at 35°C as the fuel-cell voltage was varied between open circuit and 0.5 V.

Cell temperature: 35°C; H_2 flow rate: 1.2 A/cm^2; air flow rate: 1.0 A/cm^2, ambient pressure; H_2 and air sparger temperature: 21°C.

By assuming that the cathode exhaust stream was saturated with water vapor, we estimated that the amount of water removed by evaporation could account for only about 35% of the total amount of water generated in the cathode, including the net water transported from the anode to the cathode by the combined effort of electroosmosis and back diffusion. The rest had to be removed by both capillary diffusion and gas drag force. These results show that liquid-water removal from the cathode using an interdigitated flow field and operating at this temperature (35°C) was dominated by gas-phase drag force and capillary force. Evaporation and back diffusion to the anode played only a small role. The results also show the direct effect of cathode flooding on the performance of the fuel cell. Note that whenever there were positive spikes in the cathode pressure drop there were corresponding negative spikes in the cell current density and vice versa. These results suggest that if the operating conditions (temperature, gas flow rate, current density) allow liquid water to accumulate and electrode flooding to occur, the cell performance can be affected, even at this relatively low current density (0.3 A/cm^2). In this case, the low operating temperature prevented the water produced in the cathode from being effectively removed by evaporation.

The dynamic behavior of liquid water is governed by the net accumulation rate, which is the rate of generation minus the rate of removal, and the difference between the amount of water that was initially in the electrode and that at the new steady state. Liquid-water generation rate by oxygen reduction and electroosmotic drag is almost solely controlled by current density, and, therefore, the dynamic response of the water-generation rate to changes in current density is instantaneous. On the other hand, liquid water is removed by four different mechanisms: evaporation, back-diffusion from the cathode to the anode, gas-phase drag force, and capillary force. The water removal rate by gas-phase drag force increases as the liquid water saturation increases (He et al., 2000; He and Nguyen, 2002). The water-removal rates by back diffusion and evaporation, which are small at the low temperature selected for this experiment, do not change much as long as there is still a significant amount of liquid water in the cathode backing layer. The water-removal rate by capillary force is not a simple function of liquid-water saturation, but is generally known to increase with increases in water content. As the cell was stepped back to open-circuit where

the water-generation rate was zero, the cathode pressure drop quickly decreased as the water accumulated in the backing layer was removed by all four mechanisms just described. However, as the liquid-water content in the backing layer decreased, the removal rate by gas-phase drag force and capillary force decreased, as shown by a more gradual drop in the cathode pressure drop in Figure 4. The fact that the liquid water removal rate decreased as the liquid water content decreased also suggested that gas-phase drag and capillary force played a very important role, which is in good agreement with the conclusion based on the estimation of the contribution of liquid-water removal by evaporation, as discussed before.

Note that with no electroosmotic force to overcome when the cell is at open circuit, back-diffusion for liquid water from cathode to the anode could be seen by the slight increase in the anode pressure drop. The fact that the pressure drop increase due to back-diffusion is very small suggests that liquid-water removal by back-diffusion at this operating condition plays only a small role. Finally, under these operating conditions the cathode pressure drop took about one hour to stabilize after it was put under open-circuit, which again showed that the overall liquid water transport rate was slow. The pressure drop at the end of the open-circuit step was higher than when the cell started because of liquid water entrapped in the porous backing layer that cannot be effectively removed by gas-phase drag force and capillary force. The only means of removing this last amount of water is by evaporation.

Effects of air flow rate on liquid-water removal

In a PEM fuel cell using the interdigitated flow fields, changing the air flow rate leads to changes in the liquid-water removal rates by evaporation and gas-phase drag. This increase in the air flow rate also affects the liquid water/air capillary interaction due to the change in the air-pressure field in the backing layer. When this happens, the balance between the liquid-water generation and removal rates previously observed is expected to change, leading to a new steady-state condition in the cathode backing layer. This is clearly illustrated by the results shown in Figure 5. In this three-step experiment, the cell was continuously held at 0.55 V while the air flow rate was changed from 2 A/cm^2 equivalent to 4.2 A/cm^2 and then back to 2.0 A/cm^2.

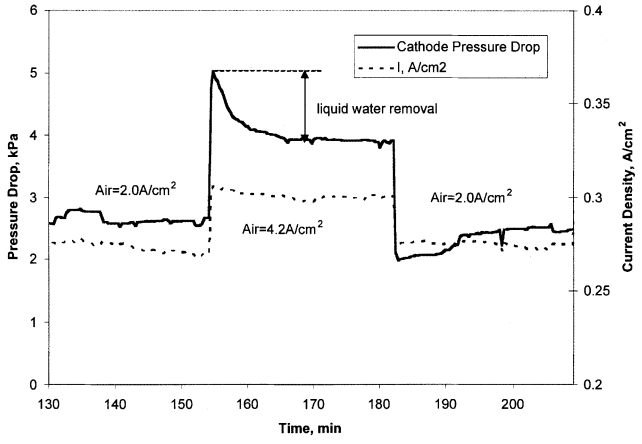

Figure 5. Effects of air flow rate on the flooding level in the cathode backing layer at cell temperature of 40°C and cell voltage of 0.55V.

H_2 flow rate: 2.0 A/cm^2, ambient pressure; H_2 sparger temperature: 43°C; air sparger temperature: 25°C

Note that during the first step when the air flow rate was set at 2 A/cm^2 the cathode pressure drop stabilized at about 2.55 kPa and the current density at 0.28 A/cm^2. As soon as the air flow was raised to 4.2 A/cm^2 two things happened. The current density increased slightly to 0.31 A/cm^2, and the cathode pressure drop increased quickly to 5.10 kPa, and then gradually decreased to about 3.93 kPa. The increase in the current density can be attributed to the higher oxygen stoichiometric flow rate and higher oxygen concentration as a result of the pressure increase in the cathode backing layer. The magnitude of the change in the current density is small compared to the change in the air flow rate. This is because the cell was held at a relatively high cell voltage of 0.55 V, at which the performance of the fuel cell was controlled more by kinetics than the mass-transport of oxygen, and was therefore not very sensitive to the enhanced mass-transport rate of oxygen induced by the higher air flow rate and better removal of liquid water.

The doubling in the cathode pressure drop is attributed to the doubling in the gas flow rate through the backing layer. Note that at this instant there was little change in the liquid-water level in the cathode's backing layer. Consequently, doubling the gas flow rate should double the pressure drop through this porous medium. However, as more water was removed from the backing layer by higher gas-phase drag force exerted by higher gas flow rate while the water generation rate stayed relatively the same, the liquid-water level in the cathode decreased, leading to a lower pressure drop across the backing layer. This explanation is supported by the behavior of the cathode pressure drop when the air flow rate was reduced back to 2 A/cm^2. One should realize that the cathode's backing layer at this instant had a lower water content than when it was at the previous 2 A/cm^2 step. Consequently, the initial pressure drop in the cathode during step three was lower than that at the end of step one. Over time as water reaccumulated in the cathode backing layer at this lower air flow rate, the pressure drop in the cathode gradually increased back to the same level as observed during step one. Note also that the initial current density during step three was slightly higher due to the same lower electrode flooding reason just given. This current density then dropped gradually back to the same level as seen during step one. This process was observed to be quite slow, showing that liquid-water transport in the backing layer is a slow process.

The effect of air flow rate is more pronounced at elevated cell temperatures and/or at low cell voltages. At higher cell temperatures, the liquid water removal rate is greatly enhanced by the higher liquid-water evaporation rate; while at lower cell voltages, the fuel cell is more sensitive to the change in the oxygen-transport rate because it operates under a mass-transport controlled regime. Figure 6 shows the responses of the cathode pressure drop and current density to a step change in the air flow rate in a PEM fuel cell operated at a constant cell voltage of 0.35 V and 50°C. The first observation is that while the air flow rate (2 A/cm^2) was the same as that of the 40°C case, the current density was much higher

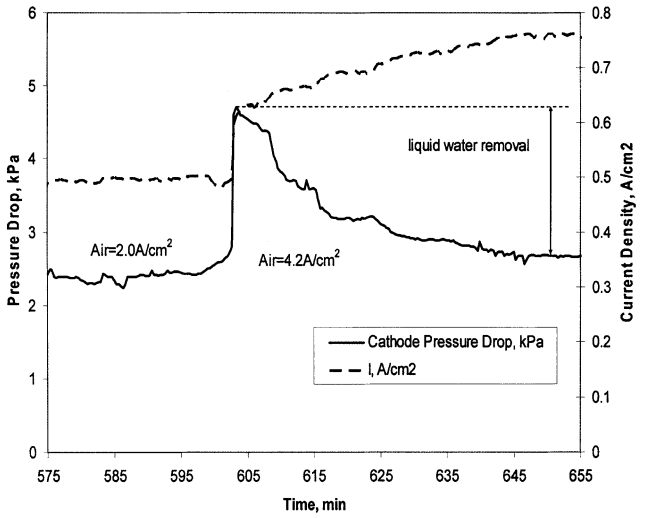

Figure 6. Effects of air flow rate on the flooding level in the cathode backing layer at cell temperature of 50°C and cell voltage of 0.35 V.

H_2 flow rate: 2.0 A/cm^2, ambient pressure; H_2 sparger temperature: 43°C; air sparger temperature: 25°C.

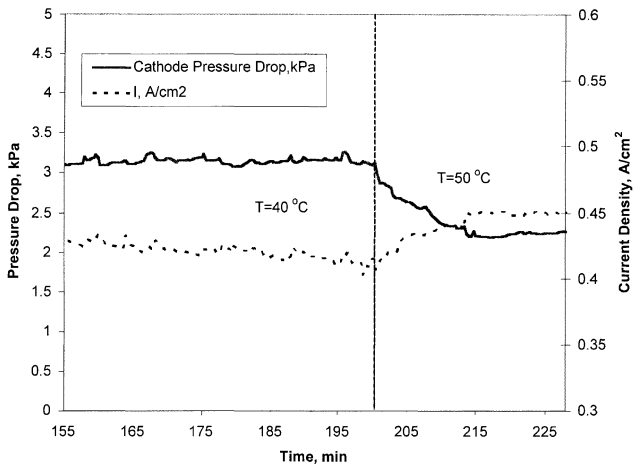

Figure 7. Effects of cell temperature on the cathode flooding level for a fuel-cell voltage at 0.45 V.

Air flow rate: 2.0 A/cm^2; H_2 flow rate: 2.0 A/cm^2, ambient pressure; H_2 sparger temperature: 43°C; air sparger temperature: 25°C.

(almost twice) and the pressure drop in the cathode was lower for the 50°C case. The better performance at 50°C can be attributed to the lower cell voltage (0.35 V vs. 0.55 V) and a higher water removal rate by evaporation, and consequently lower water content in the cathode backing layer due to the fact that the water vapor pressure at 50°C is almost double that at 40°C.

Next, similar to the behavior observed in Figure 5 for the case at 40°C, the cathode pressure drop first doubled, then gradually decreased and approached a new steady state. However, there are three differences in the responses in this run as compared to the previous run. First, the initial increase in the current density is much larger and can be attributed to a higher sensitivity to the change in oxygen concentration at lower cell voltages and higher cell temperatures. Second, instead of staying relatively constant as in the 40°C case, the current density continued to increase, corresponding to the change of liquid-water content. This again is due to the higher sensitivity to the change in oxygen transport caused by the change in liquid-water saturation. Third, the new steady-state pressure drop was not much higher than that at the lower gas flow rate even though the current density is 50% higher, showing that a significant amount of liquid water had been removed by the higher evaporation rate. The different responses observed at 50°C as compared to those observed at 40°C can be attributed to the higher water removal rate by evaporation at elevated temperatures and its greater effect on the total liquid-water removal rate.

Effects of cell temperatures on liquid-water removal

In this study, an experiment was conducted in which the air flow rate was kept the same and only the fuel-cell temperature was changed. This was done to isolate the effect of the operating temperature on the pressure-drop response in the cathode backing layer. The experiment was conducted as follows. The fuel cell was held at 40°C and allowed to reach steady state. Next, the fuel-cell temperature was quickly ramped to 50°C and the current density and cathode pressure drop were monitored until a new steady state was reached. The cell voltage was held constant at 0.45 V during the entire run. Note that since the heat capacity of the fuel cell was small compared to the heating power of the heater used, the cell temperature reached its new temperature setting in less than half a minute. This temperature delay is considered insignificant compared to the slow transient process of liquid-water response (in a time scale of about 20 min). The results obtained for this run are given in Figure 7.

As can be expected, the cathode pressure drop decreased after the cell temperature increased, confirming that less liquid water was presented in the backing layer due to the higher liquid-water removal rate. There are several factors related to the increase in cell temperature that contributed to higher liquid-water removal. Higher water-vapor pressure at higher temperature led to a higher liquid-water evaporation rate. Another factor was that for the same mass flow rate of air, a higher cell temperature resulted in a higher volumetric flow rate (that is, velocity) in the backing layer, which led to a higher removal rate of liquid water by gas-phase drag (He et al., 2000; Nguyen and He 2002). The surface tension and viscosity of liquid water also decreased as the temperature increased, which would allow liquid-water to be flushed out more easily.

Finally, note that the current density increased a little bit after the step increase in the cell temperature. However, the net gain of the current density in this case was not as big as that in Figure 6 due to the difference in the air stoichiometry and cell voltage. At this cell voltage, 0.45 V vs. 0.35 V for the previous case, the cell is under more kinetic control and less transport control. Consequently, any effect on transport is lessened in this case. In this run, the cell only benefited from higher water-vapor pressure and not from higher mass flow rate, as in the two previous runs. This response also confirms that liquid-water removal from the cathode is a slow process.

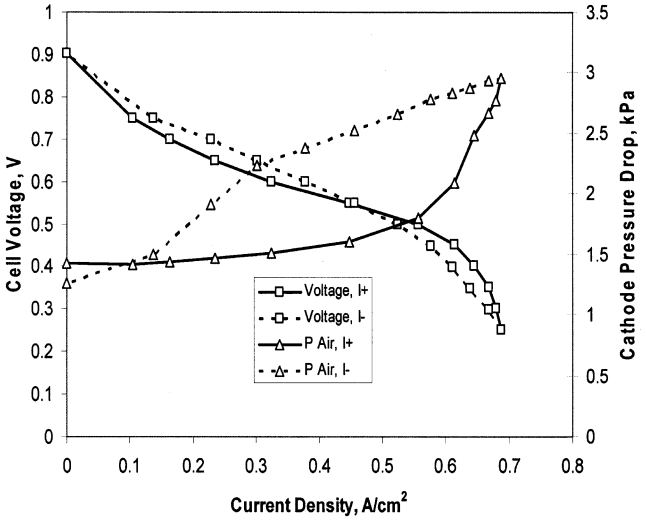

Figure 8. Hysteresis behavior of liquid water in the cathode porous backing layer.

Cell temperature: 51°C; H_2 flow rate: 2.0 A/cm^2, air flow rate: 2.8 A/cm^2, ambient pressure; H_2 sparger temperature: 50°C; air sparger temperature: 27°C.

Hysteresis behavior of liquid water in the porous backing layer

It has long been recognized that during a polarization scan of a PEM fuel cell, the downward scan (higher current density or lower cell voltage direction) curve is usually different from that of the upward scan (lower current density or higher voltage direction). Typical downward ($I+$) and upward ($I-$) polarization curves and the corresponding cathode pressure-drop curves for our fuel cell are shown in Figure 8. Note that during the downward scan liquid-water content in the cathode porous backing layer increased as the water-generation rate controlled by the current density increased. We refer to this half-cycle as the water-imbibition cycle (Leverett, 1941). During the upward scan, as the current density went from high to low, the same happened to the liquid-water content. We call this half-cycle the water-drainage cycle (Leverett, 1941).

The results given in Figure 8 showed that at the same cathode pressure drop, which could be interpreted as being at the same liquid-water saturation level, the liquid-water removal rate could support a higher current-density or water-generation rate in the imbibition cycle than that in the drainage cycle for most of the cathode pressure drops tested. This suggested that at the same liquid-water saturation level, the liquid-water removal rate was faster in the imbibition cycle. Because the cell temperature and the gas flow rate were constant during the run, the liquid-water removal rates by evaporation and gas-phase drag were also constant for a given liquid-water saturation level. The differences in the liquid-water removal rate stemmed from the hysteresis of the capillary pressure and liquid saturation level in porous media (Leverett, 1941). This hysteresis is attributed to the complicated geometric configuration of the pore networks in a porous medium. The cause of the hysteresis behavior has been discussed in detail by Smith (1933). It was found that for a given average water saturation level, many stable liquid water distributions exist (Smith, 1933). The same hysteresis behavior is observed in the porous electrodes of a PEM fuel cell. However, no experimental data of capillary curves are available for carbon paper or carbon cloth used in PEM fuel cells. Our research group is currently developing experiments to obtain these data for the materials used in PEM fuel cells, and the results will be integrated with our two-phase model (He et al., 2000; He and Nguyen, 2002) to quantify the amount of liquid water in backing layers. The results will be presented in the near future.

Finally, it is important to point out that the polarization curves for imbibition and drainage cycles showed many complicated characteristics. Evidently, the polarization curves could not be completely explained by the pressure-drop data. This is because of the variations in the Nafion membrane conductivity with different water content and distribution. Besides intrinsic catalysts activity, catalysts utilization, and oxygen transport, ionic conductivity is another big factor in controlling cell performance. At current densities higher than 0.45 A/cm^2, the cell performed better in the imbibition cycle, mostly due to lower flooding. At lower current densities, better performance in the drainage cycle can be attributed to higher ionic conductivity due to higher water contents in the membrane.

In summary, the fact that the results of the effects of cell temperature and gas flow rates on the liquid-water removal are as expected strongly supports the diagnostic tool presented here as a valid and valuable tool. The transient pressure drop and hysteresis behavior are new and very interesting. This knowledge will become extremely useful in the understanding of the transport of liquid water in the gas diffusion layer and its effect on the transient behavior of PEM fuel cells. Furthermore, this diagnostic tool can be used to study the effect of various wetting and water-transport characteristics of gas-diffusion layers on the water accumulation, removal rate, and dynamics in the electrodes of PEM fuel cells. Knowledge from this study can be used to develop gas-diffusion layers with optimal water removal properties.

As with any tools, this diagnostic tool has limitations. Currently, this tool can only be applied to PEM fuel cells using interdigitated flow fields. Second, it can only detect flooding occurring within gas-diffusion layers (or backing layers). Flooding within the catalyst layers cannot be detected by this diagnostic tool. A new diagnostic tool that can separate the total voltage loss in a fuel cell into voltage loss by individual components and detect flooding in the catalyst layers is currently under development. The results from this work will be presented in the future. Finally, even though the results presented here apply to fuel cells that use interdigitated flow fields, any knowledge resulting from this work that can be used to improve the water-removal rate from the gas-diffusion layers will benefit PEM fuel cells using other flow-field designs.

Conclusions

An electrode flooding monitoring device designed for PEM fuel cells with interdigitated flow distributors was proposed and tested. The pressure drop between inlet and outlet channels can be used as a diagnostic signal to monitor the liquid water content in the porous electrodes, because of the strong

dependence of the gas permeability of the porous electrodes on the liquid-water content. The device has been employed to investigate the correlation between the fuel-cell performance and (1) the liquid-water saturation level at various operating conditions, and (2) the dynamics and hysteresis behavior of liquid water in the electrode backing layers. Several key operation parameters that strongly affect liquid-water removal were also studied. The following conclusions have been drawn:

(1) The monitoring device can be used with no modification to existing fuel-cell assembly to give real-time flooding information in the electrode backing layers during operation.

(2) For the first time, direct evidence is provided to show that inadequate water removal causes liquid-water buildup in the cathode, which in excessive amounts can severely reduce the fuel-cell performance.

(3) Liquid-water transport processes are slow. When a PEM fuel cell undergoes large step-changes in current density, the cell could take more than 30 min. to reach a new steady state.

(4) Increasing air flow rate or cell temperature helps liquid-water removal. This observation is well known to researchers in the fuel-cell area. However, the pressure-drop data allow the effect of temperature and air flow rate on the water-removal rate to be observed in a PEM fuel cell in real time during operation.

(5) Net liquid water back-diffusion from the cathode to the anode is confirmed. This effect has been suspected by researchers in the area for a long time, and was confirmed only by conducting a total water balance on the cell. This diagnostic tool allows this phenomenon to be observed in a fuel cell during operation in real time.

(6) The hysteresis behavior of fuel-cell performance during water imbibition and drainage cycle is attributed to the difference in water-removal rate by capillary force and the difference in membrane conductivity.

Acknowledgments

This work was supported by the National Science Foundation under Grant No. CTS-9803364.

Literature Cited

He, W., and T. V. Nguyen, "A New Diagnostic Tool for Liquid Water Management in PEM Fuel Cells Using Interdigitated Flow Fields," Electrochemical Society Meeting, Philadelphia, PA (2002).

He, W., J. S. Yi, and T. V. Nguyen, "Two-Phase Flow Model of the Cathode of PEM Fuel Cells Using Interdigitated Flow Fields," *AIChE J.*, **46**, 2053 (2000).

Kaviany, M., *Principles of Heat Transfer in Porous Media*, 2nd Ed., Springer, NY, 489 (1995).

Leverett, M. C., "Capillary Behavior in Porous Solids," *Pet. Trans. AIME*, **142**, 152 (1941).

Natarajan, D., and T. V. Nguyen, "A Two-Dimensional, Two-Phase, Multi-Component, Transient Model for the Cathode of a PEM Fuel Cell Using Conventional Gas Distributors," *J. Electrochem. Soc.*, **148**, 1324 (2001).

Nguyen, T. V., "A Gas Distributor Design for Proton-Exchange-Membrane Fuel Cells," *J. Electrochem. Soc.*, **143**, L105 (1996).

Nguyen, T. V. and W. He, "Interdigitated Flow Field Design: Experimental Results and Theoretical Calculations," *Handbook of Fuel Cell Technology: Fuel Cell Technology and Applications*, Vol. III, W. Vielstich, H. Gasteiger, and A. Lamm, eds., Wiley, New York (2003).

Nguyen, T. V., J. Mitchell, and W. He, "Monitoring and Controlling Electrode Flooding in PEM Fuel Cells," AIChE Meeting, Reno, NV (2001).

Nguyen, T. V., and R. E. White, "A Water and Heat Management Model for Proton-Exchange-Membrane Fuel Cells," *J. Electrochem. Soc.*, **140**, 2178 (1993).

Smith, W. O., "The Final Distribution of Retained Liquid in an Ideal Uniform Soil," *Physics*, **4**, 425 (1933).

Wang, Z. H., C. Y. Wang, and K. S. Chen, "Two Phase Flow and Transport in the Air Cathode of Proton Exchange Membrane Fuel Cells," *J. Power Sources*, **94**, 40 (2001).

Whitaker, S., "Flow in Porous Media II: The Governing Equations for Immiscible, Two-Phase Flow," *Transp. Porous Media*, **1**, 105 (1986).

Woods, D., III, J. Yi, and T. V. Nguyen, "Effect of Direct Liquid Water Injection and Interdigitated Flow Field on the Performance of Proton Exchange Membrane Fuel Cells," *Electrochim. Acta*, **43**, 3795 (1998).

Yi, J. S., and T. V. Nguyen, "The Effect of the Flow Distributor of the Performance of PEM Fuel Cells," *Proc. on Proton Conducting Membrane Fuel Cells*, The Electrochemical Society, Pennington, NJ, p. 66 (1995).

Manuscript received Sept. 10, 2002, and revision received Apr. 15, 2003.